北京理工大學
BEIJING INSTITUTE OF TECHNOLOGY

Ab Initio calculation of Electron Temperature Dependent Heat Capacity and Electron-Phonon Coupling Factor of Noble Metals

Reporter: Yongnan Li

Date: 25/6/2022

Femtosecond laser

Laser energy deposited in the electron subsystem

Nonequilibrium state
High T_e
Room Temperature T_l

Electron-Phonon interaction

Electrons and lattice equilibrate to same temperature

Two temperature model (TTM)

$$C_e \frac{\partial T_e}{\partial t} = \nabla(\kappa_e \nabla T_e) - G_{e-ph}(T_e - T_l) + S$$

$$C_l \frac{\partial T_l}{\partial t} = \nabla(\kappa_l \nabla T_l) + G_{e-ph}(T_e - T_l)$$

- Electron Heat Capacity C_e
- Lattice Heat Capacity C_l
- Electron-Phonon Coupling Factor G_{e-ph}

Noble Metals

- Used as catalysts
- Advanced hydrogen storage capacity
- Producing hydrogen polymer electrolyte fuel cell
- **Getting more contact area as nanoparticles**

Generate nanoparticles with femtosecond laser

	Electron Structure	
Gold (Au)	$6s^1 5d^{10}$	Filled *d* block
Palladium (Pd)	$4d^{10}$	
Iridium (Ir)	$6s^2 5d^7$	Partially-filled *d* block
Rhodium (Rh)	$5s^1 4d^8$	

Focusing on material parameters for TTM

Calculation Method

北京理工大学 BEIJING INSTITUTE OF TECHNOLOGY

Electron Heat Capacity

$$C_e\Big|_{T_e} = \left(\frac{\partial E_{int}|_{T_e}}{\partial T_e}\right)_V = \int_{-\infty}^{+\infty}\left(g(\varepsilon)\Big|_{T_e}\frac{\partial f(\varepsilon)|_{T_e}}{\partial T_e} + f(\varepsilon)\Big|_{T_e}\frac{\partial g(\varepsilon)|_{T_e}}{\partial T_e}\right)\varepsilon d\varepsilon$$

Lattice Heat Capacity

$$C_l\Big|_{T_e,T_l} = \left(\frac{\partial E_{vib}|_{T_e,T_l}}{\partial T_l}\right)_V = \int_{-\infty}^{+\infty} D(\omega)\Big|_{T_e}\frac{\partial n(\omega)|_{T_l}}{\partial T_l}\omega d\omega$$

Electron-Phonon Coupling Factor

$$G_{e-ph}\Big|_{T_e} = \frac{\pi\hbar k_B\lambda\langle\omega^2\rangle}{g(\varepsilon_F)|_{T_e}}\int_{-\infty}^{+\infty}\left[g(\varepsilon)\Big|_{T_e}\right]^2\left(-\frac{\partial f(\varepsilon)|_{T_e}}{\partial\varepsilon}\right)d\varepsilon$$

Fermi-Dirac Distribution Function f chemical potential μ

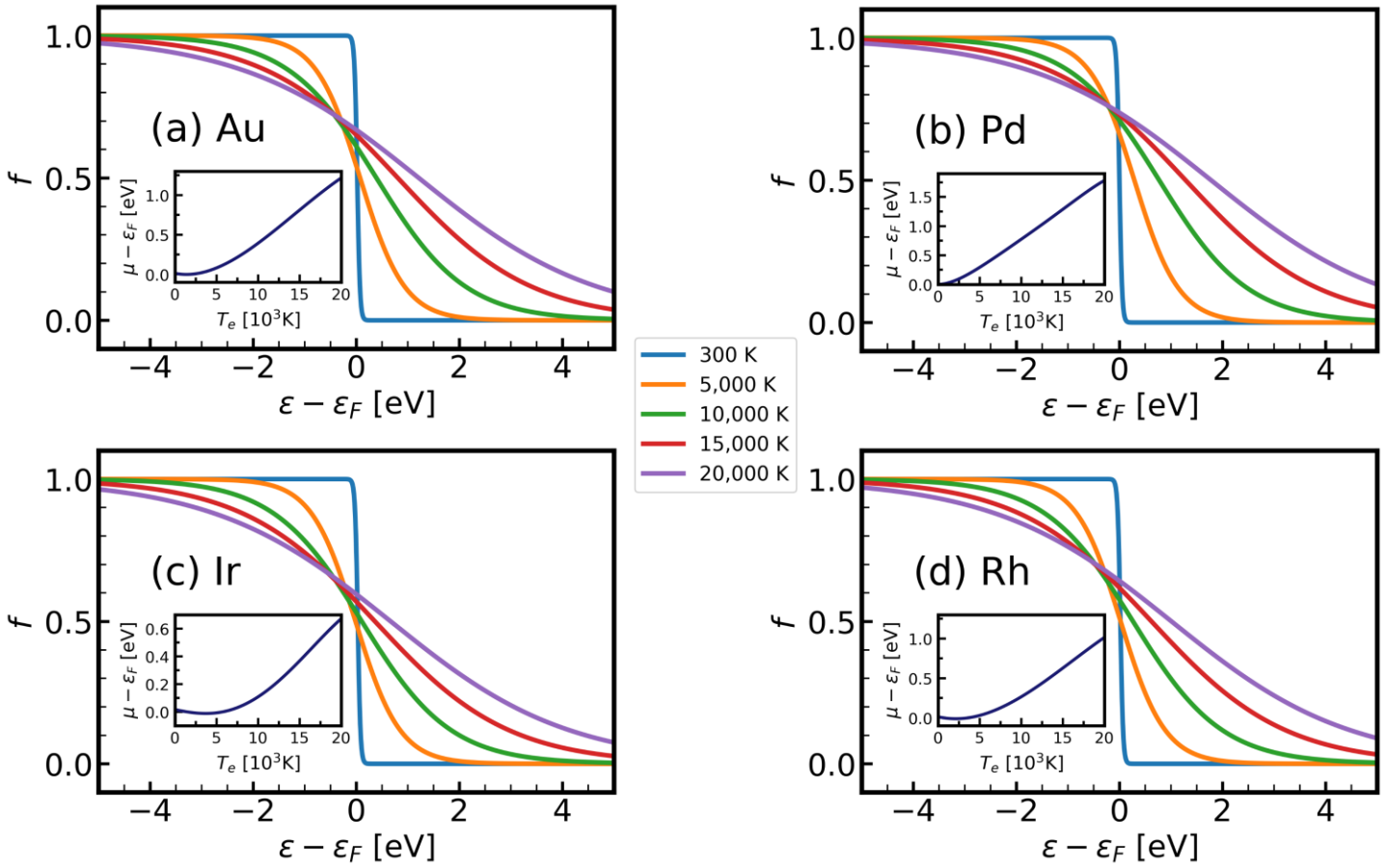

T_e

Smearing of f

Increase of μ

Fig. 1 Electron temperature T_e dependent f for (a) Au, (b) Pd, (c) Ir, and (d) Rh. Insets of (a)-(d) depict the changes of chemical potential μ to the Fermi energy ε_F, which affect the variations of f.

Electron Density of States g

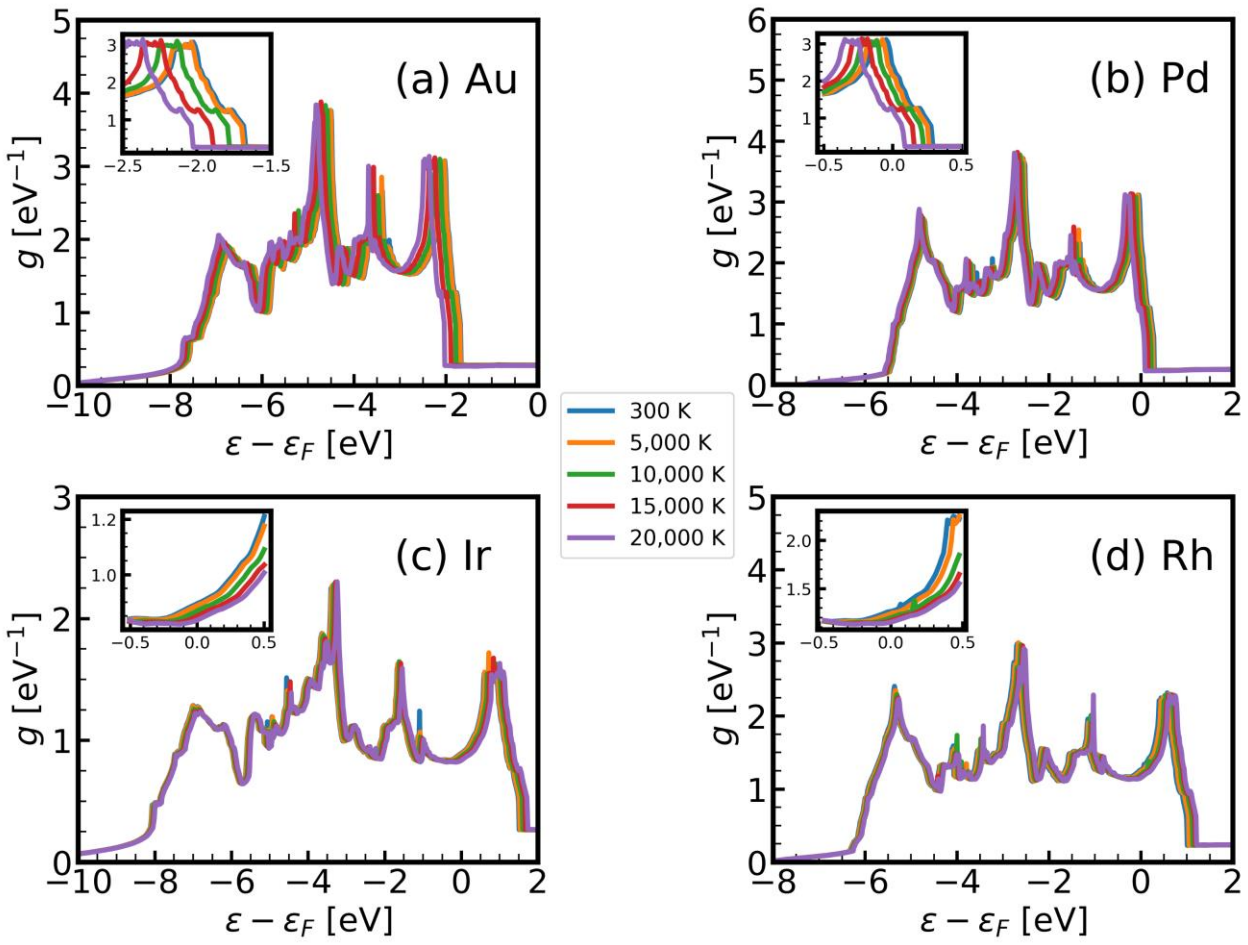

Fig. 2 Electron density of states g for (a) Au, (b) Pd, (c) Ir, and (d) Rh for electron temperature T_e at 300 K, 5,000 K, 10,000 K, 15,000 K and 20,000 K.

Filled *d* block

d block delocalization

↓

Left shift

Partially-filled *d* block

d block localization

↓

Right shift

Electron Heat Capacity C_e

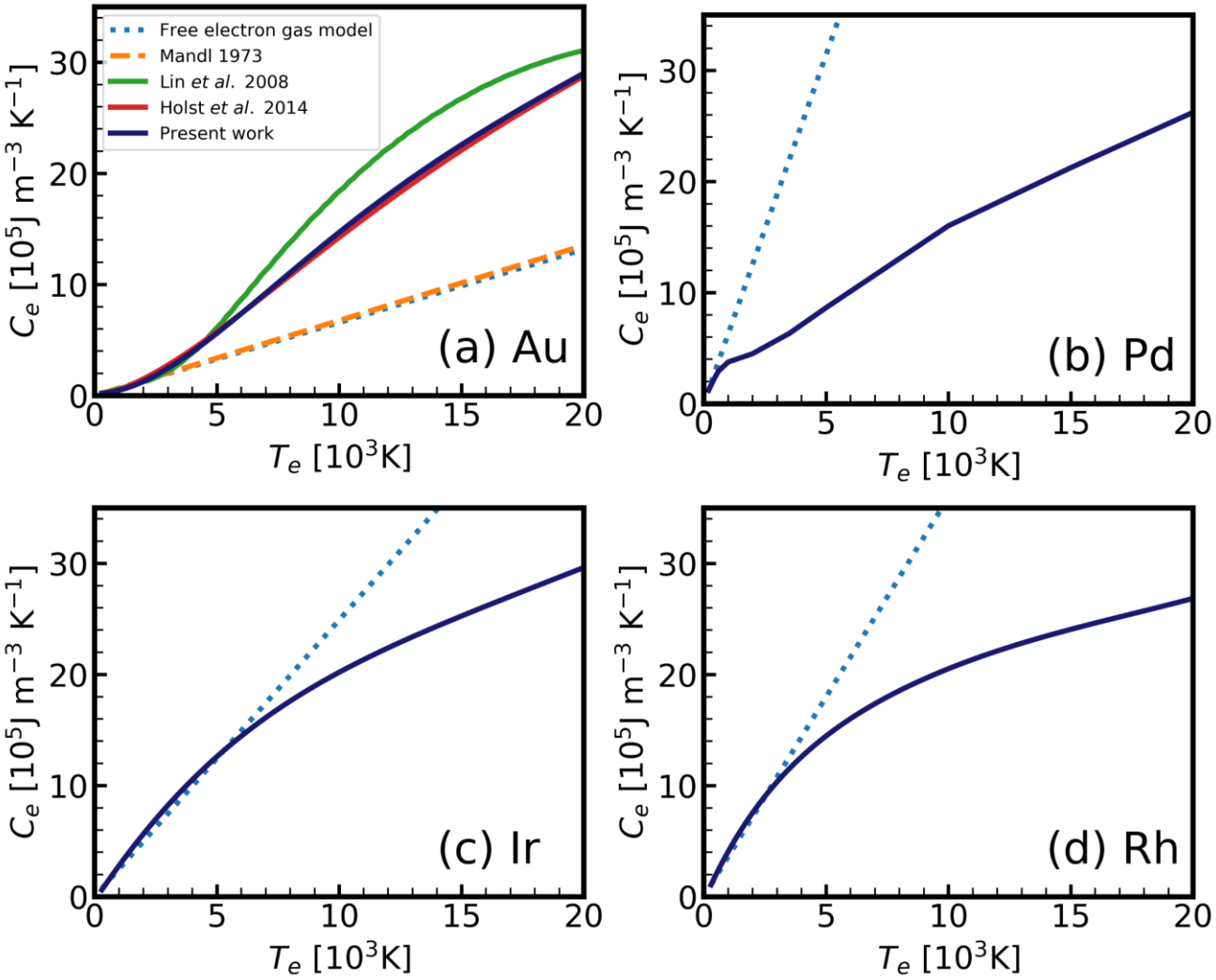

$$C_e\Big|_{T_e} = \left(\frac{\partial E_{int}|_{T_e}}{\partial T_e}\right)_V$$
$$= \int_{-\infty}^{+\infty}\left(g(\varepsilon)\Big|_{T_e}\frac{\partial f(\varepsilon)|_{T_e}}{\partial T_e} + f(\varepsilon)\Big|_{T_e}\frac{\partial g(\varepsilon)|_{T_e}}{\partial T_e}\right)\varepsilon d\varepsilon$$

Fig. 3 Electron temperature T_e dependent electron heat capacity C_e for (a) Au, (b) Pd, (c) Ir, and (d) Rh. The curves are compared with several theoretical calculations and experimental results. For (a) Au: dotted line for linear factor $\gamma = \pi^2 k_B^2 g(\varepsilon_F)/3$ from the free electron gas model, dashed line for the linear factor $\gamma = 67.6$ Jm^{-3}K^{-2} from experiment [1], the calculation results by Holst *et al.* [2] and Lin *et al.* [3] are shown. For (b) Pd, (c) Ir and (d) Rh: dotted line for linear factor $\gamma = \pi^2 k_B^2 g(\varepsilon_F)/3$ from free-electron-gas model.

[1] F. Mandl, Phys. Bull. **24** (1973) 492.
[2] B. Holst *et al.*, Phys. Rev. B. **90** (2014) 1–9.
[3] Z. Lin *et al.*, Phys. Rev. B. **77** (7) (2008).

Electron-Phonon Coupling Factor G_{e-ph}

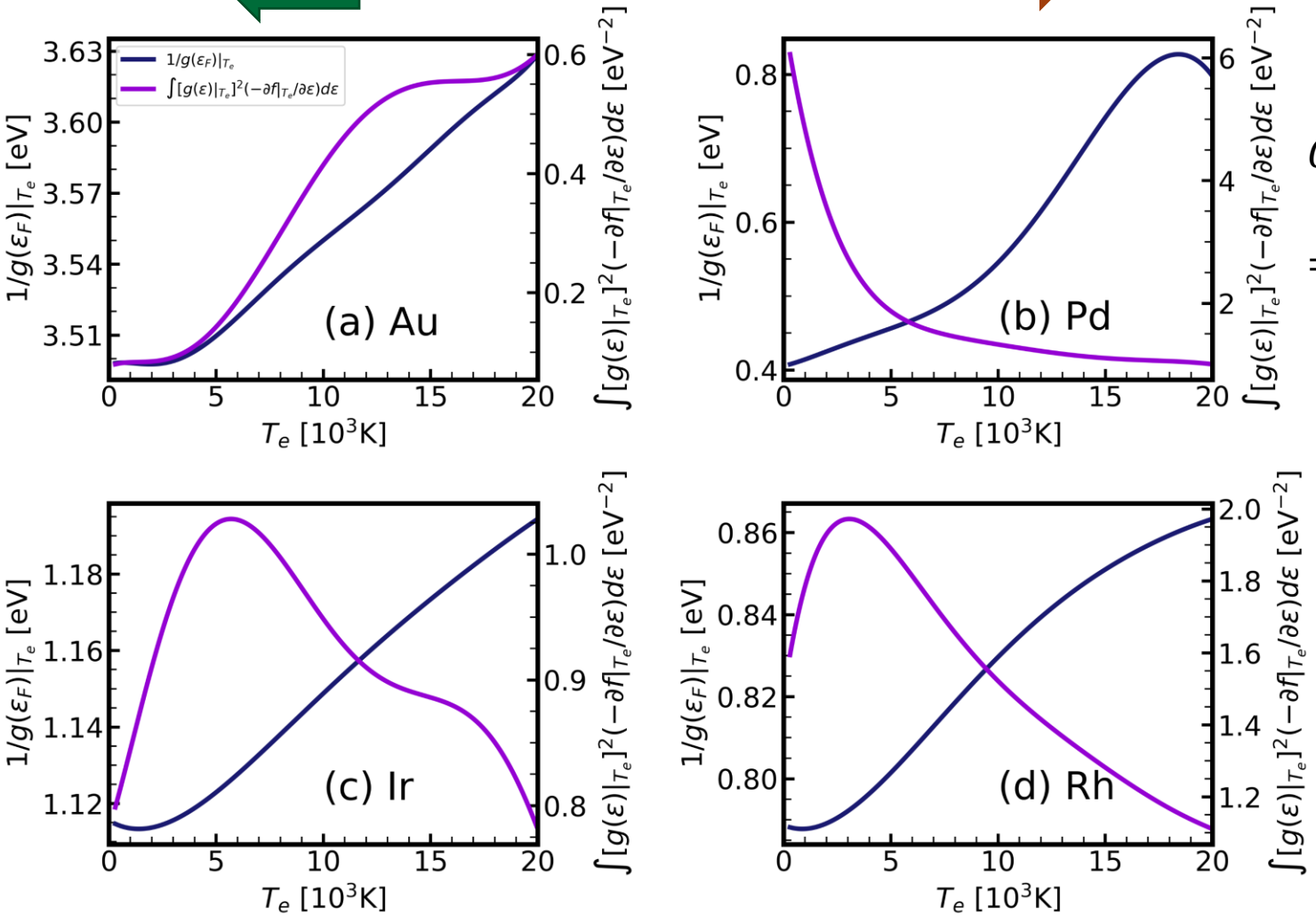

$$G_{e-ph}\Big|_{T_e} = \frac{\pi\hbar k_B\lambda\langle\omega^2\rangle}{g(\varepsilon_F)|_{T_e}}\int_{-\infty}^{+\infty}\left[g(\varepsilon)\Big|_{T_e}\right]^2\left(-\frac{\partial f(\varepsilon)|_{T_e}}{\partial\varepsilon}\right)d\varepsilon$$

Fig. 4 The variations of the reciprocal of electron temperature T_e dependent electron density of states g at $\varepsilon = \varepsilon_F$ and the variations of the integral $\int_{-\infty}^{+\infty}[g(\varepsilon)|_{T_e}]^2\left(-\frac{\partial f(\varepsilon)|_{T_e}}{\partial\varepsilon}\right)d\varepsilon$ with T_e in Eq. (7) for (a) Au, (b) Pd, (c) Ir, and (d) Rh.

Electron-Phonon Coupling Factor G_{e-ph}

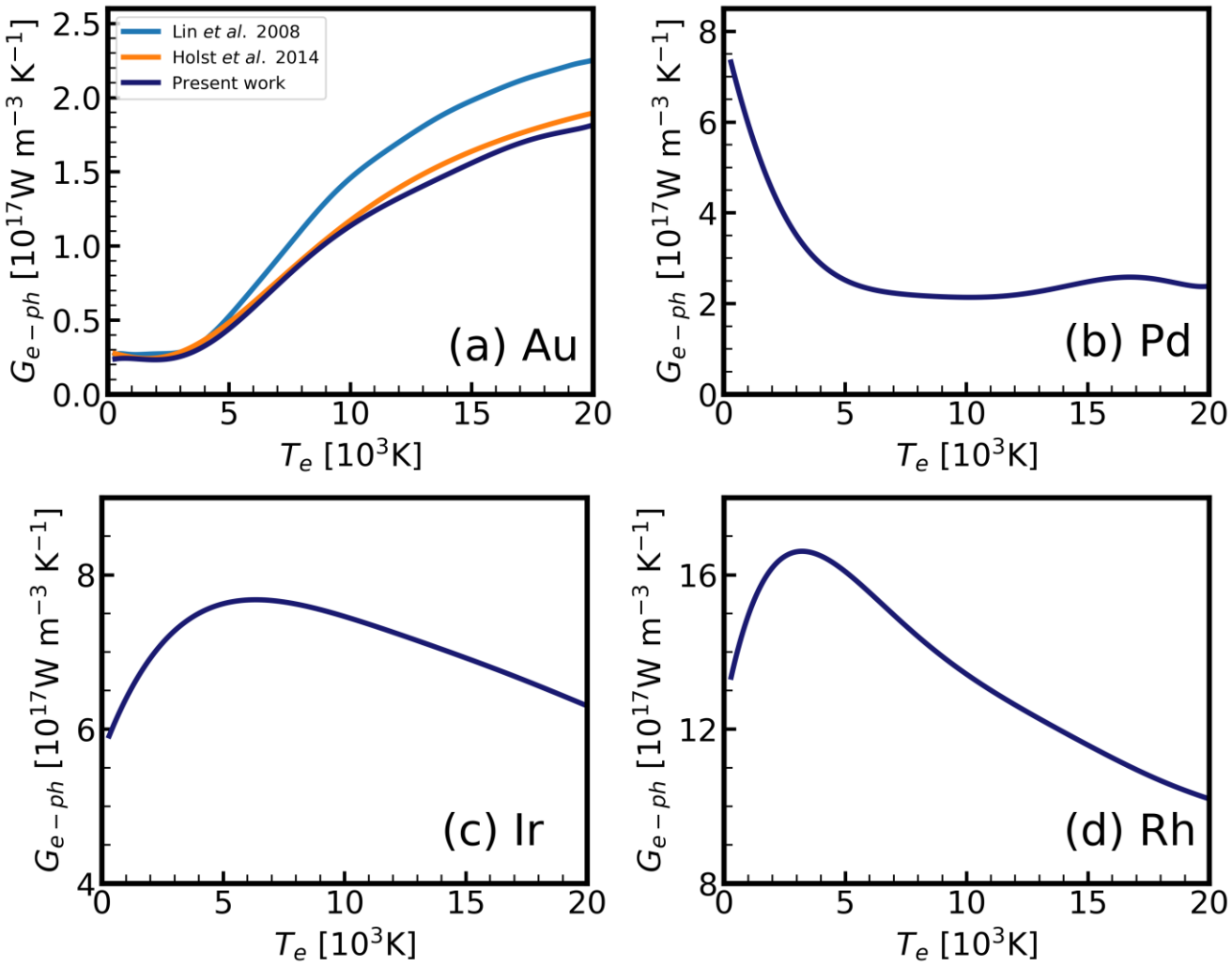

$$G_{e-ph}\Big|_{T_e} = \frac{\pi\hbar k_B \lambda\langle\omega^2\rangle}{g(\varepsilon_F)|_{T_e}} \int_{-\infty}^{+\infty} \left[g(\varepsilon)\Big|_{T_e}\right]^2 \left(-\frac{\partial f(\varepsilon)|_{T_e}}{\partial\varepsilon}\right) d\varepsilon$$

Fig. 5 Electron temperature T_e dependent electron-phonon coupling factor G_{e-ph} for (a) Au, (b) Pd, (c) Ir, and (d) Rh. For (a) Au, the curve is compared with several theoretical calculations, the calculation results by Holst *et al.* [1] and Lin *et al.* [2] are shown.

[1] B. Holst *et al.*, Phys. Rev. B. **90** (2014) 1–9.
[2] Z. Lin *et al.*, Phys. Rev. B. **77** (7) (2008).

Phonon Density of States D

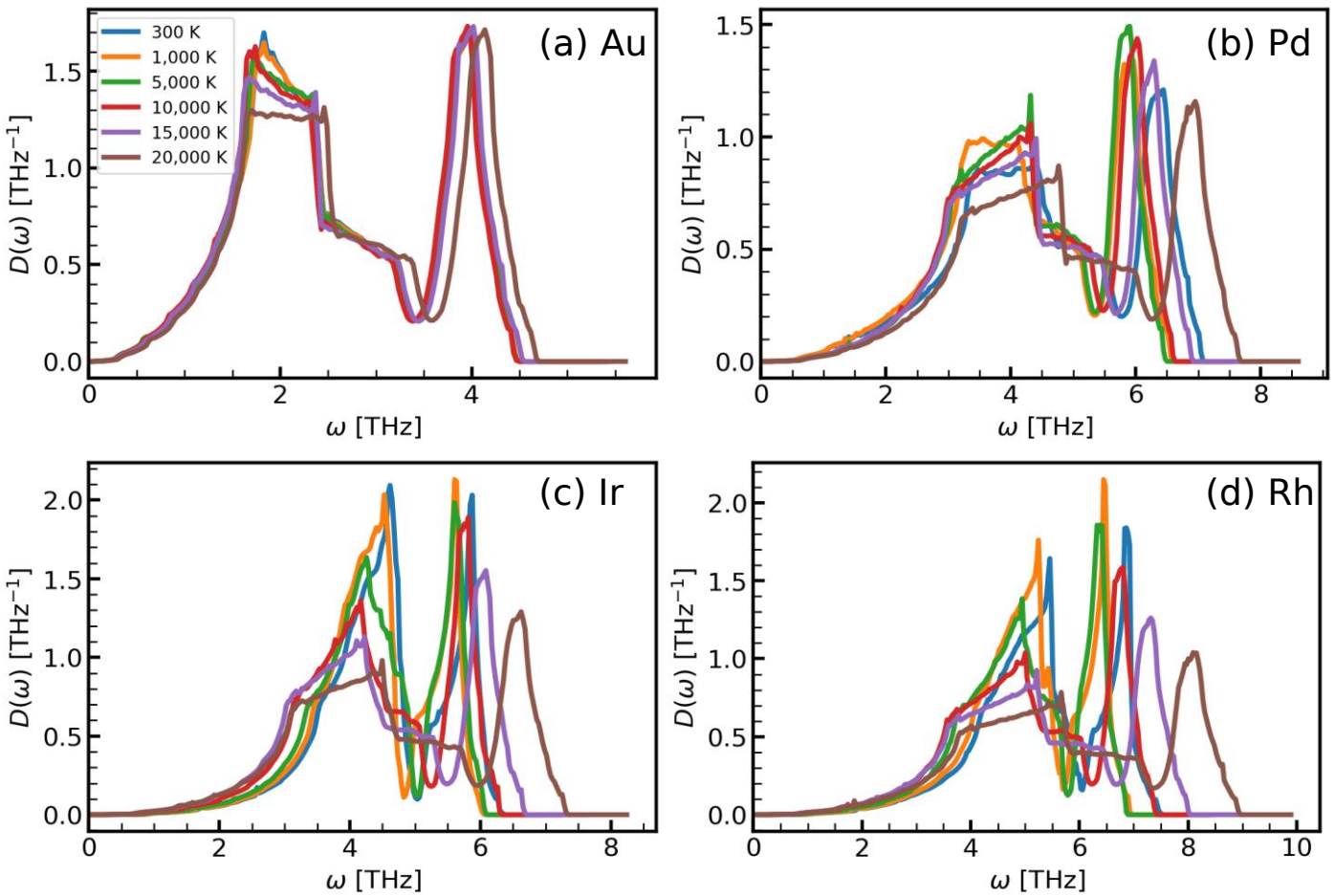

T_e

Smearing of D

Fig. 6 Phonon density of states g for (a) Au, (b) Pd, (c) Ir, and (d) Rh for electron temperature T_e at 300 K, 5,000 K, 10,000 K, 15,000 K and 20,000 K.

Lattice Heat Capacity C_l

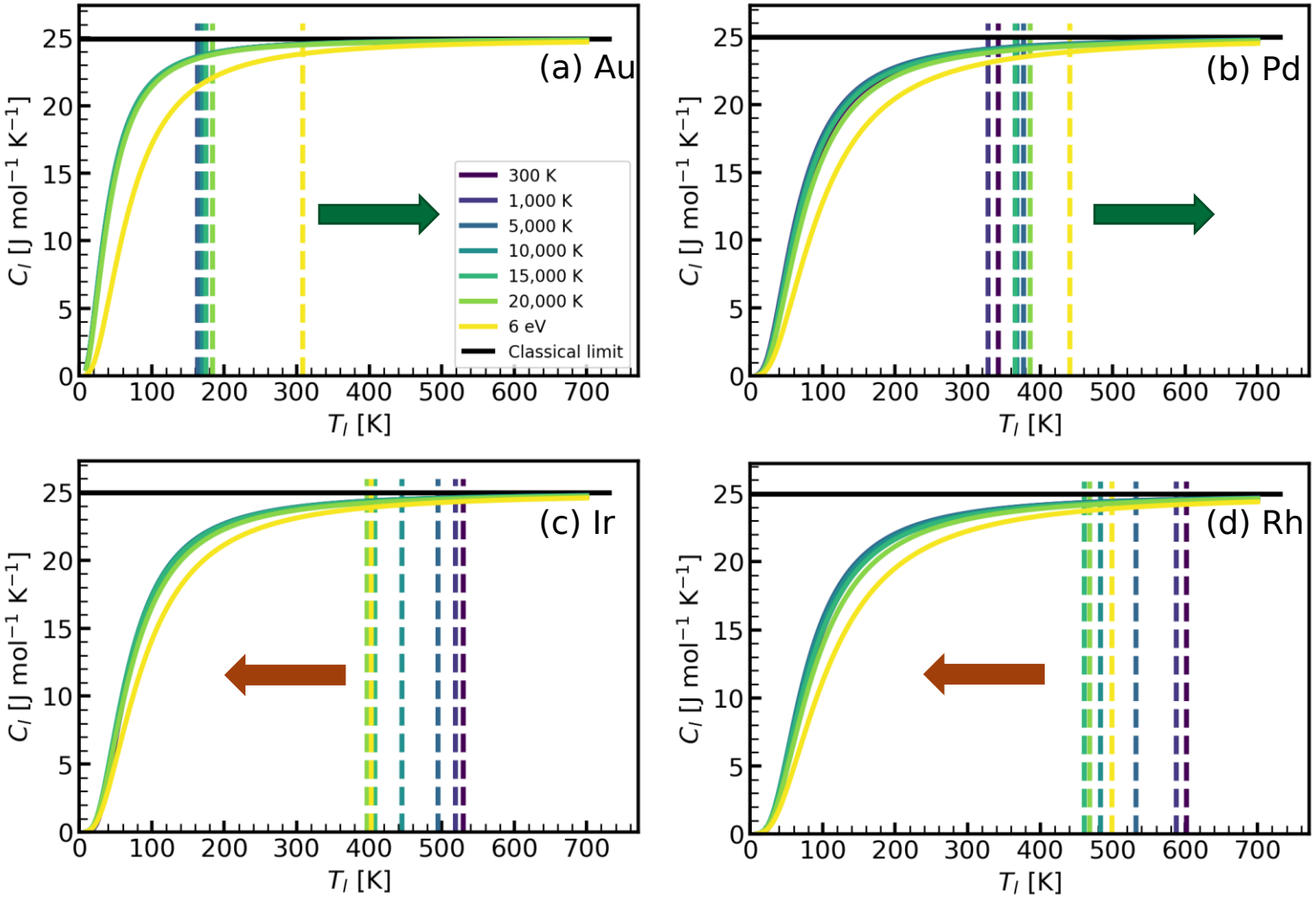

$$C_l\Big|_{T_e,T_l} = \int_{-\infty}^{+\infty} D(\omega)\Big|_{T_e} \frac{\partial n(\omega)|_{T_l}}{\partial T_l}\omega d\omega$$

Fig. 7 Electron temperature T_e dependent lattice heat capacity C_l for (a) Au, (b) Pd, (c) Ir, and (d) Rh. Vertical dotted lines indicates to the corresponding Debye temperature Θ_D. Obviously, the result is consistent to classical limit 24.94 J mol^{-1} K^{-1}.

Debye Temperature Θ_D

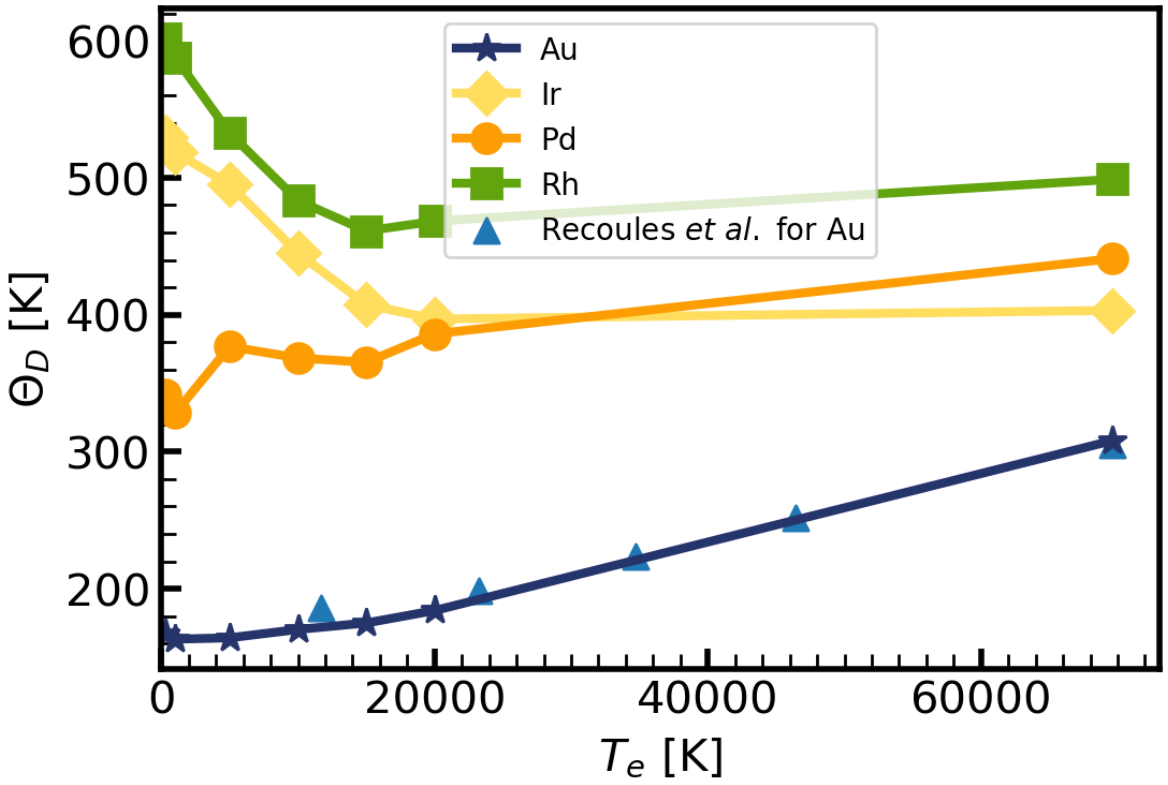

Fig. 8 Electron temperature T_e dependent Debye Temperature Θ_D for (a) Au, (b) Pd, (c) Ir, and (d) Rh.
The theoretical calculation result for Au by Recoules *et al.* [1].

[1] V. Recoules *et al.*, Phys. Rev. Lett. **96** (2006) 1–4.

Phonon Dispersion Curves

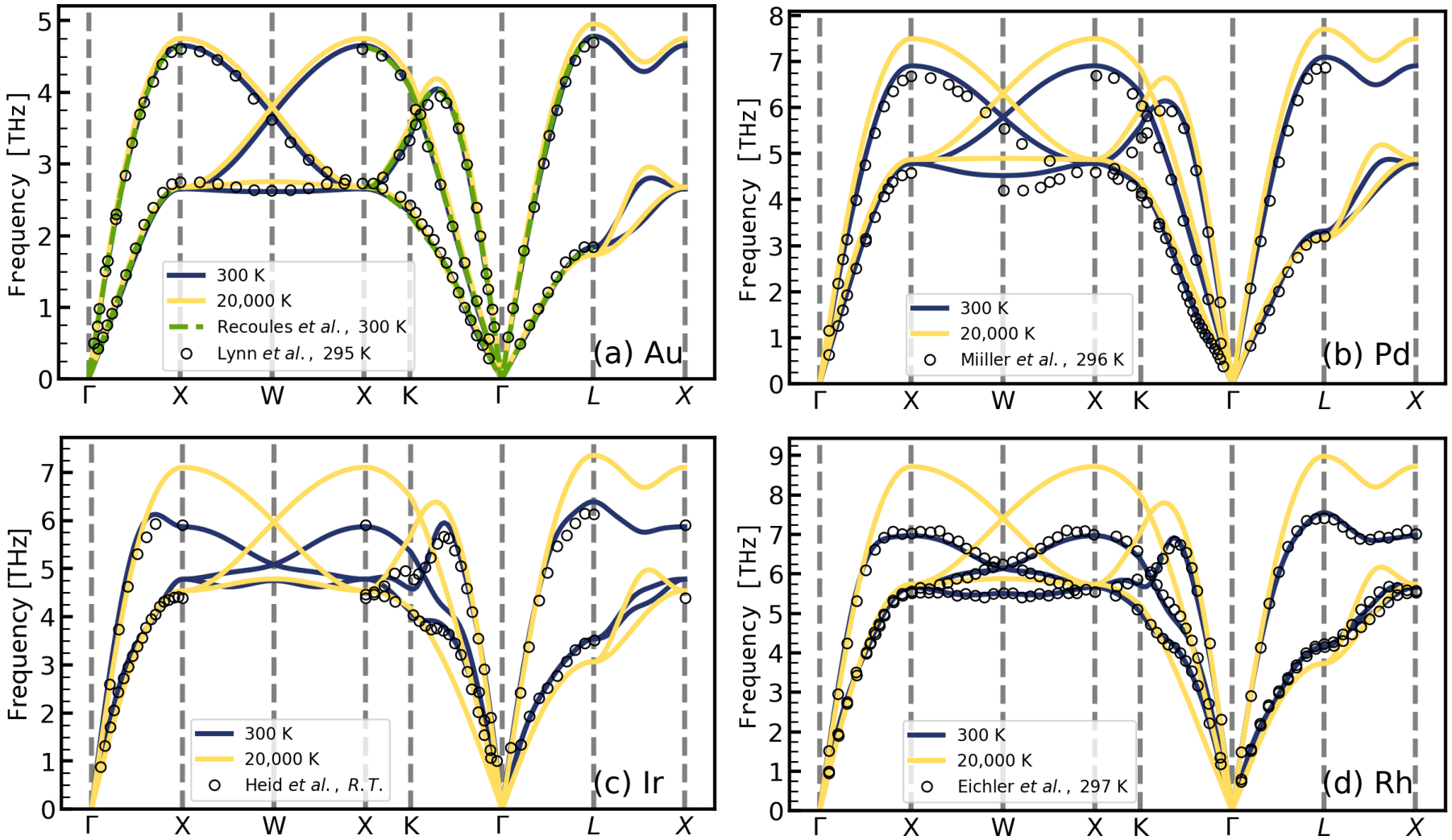

Fig. 9 Electron temperature T_e dependent Phonon dispersion curves for (a) Au, (b) Pd, (c) Ir, and (d) Rh, the curves are compared with experimental results. Circle symbols for Lynn *et al.* [1], Miiller *et al.* [2], Heid *et al.* [3], Eichler *et al.* [4] for (a) Au, (b) Pd, (c) Ir, and (d) Rh, respectively. Theoretical calculation result by Recoules *et al.* [5].

[1] J.W. Lynn *et al.*, Phys. Rev. B **8**, 3493 (1973).
[2] A.P. Miiller *et al.*, Phys. Rev. Lett. **20** (1968) 798.
[3] R Heid *et al.*, J. Phys.: Condens. Matter **10** (1998) 7967.
[4] A. Eichler *et al.*, Phys. Rev. B **57**, 324 (1973).
[5] V. Recoules *et al.*, Phys. Rev. Lett. **96** (2006) 1–4.

Conclusion

北京理工大学 BEIJING INSTITUTE OF TECHNOLOGY

Ab Initio Calculation

- Electron Heat Capacity C_e
- Lattice Heat Capacity C_l
- Electron-Phonon Coupling Factor G_{e-ph}

Electrons Transitions

Phonon Response

Generate nanoparticles with femtosecond laser

北京理工大學
BEIJING INSTITUTE OF TECHNOLOGY

THANK YOU FOR YOUR ATTENTION

Reporter: Yongnan Li Date: 25/6/2022